RAA 2016 Vol. **16** No. **8**, 124 (10pp) doi: 10.1088/1674–4527/16/8/124
http://www.raa-journal.org *http://iopscience.iop.org/raa*

Research in Astronomy and Astrophysics

Acceleration feedback control (AFC) enhanced by disturbance observation and compensation (DOC) for high precision tracking in telescope systems

Qiang Wang[1,2], Hua-Xiang Cai[1,2,3], Yong-Mei Huang[1], Liang Ge[4], Tao Tang[1,2], Yan-Rui Su[1,2,3], Xiang Liu[1,2], Jin-Ying Li[1,2], Dong He[1,2], Sheng-Ping Du[1,2] and Yu Ling[1,2]

[1] Institute of Optics and Electronics, Chinese Academy of Sciences, Chengdu 610209, China; *wangqiang_mailbox@yeah.net*
[2] Key Laboratory of Optical Engineering, Chinese Academy of Sciences, Chengdu 610209, China
[3] University of Chinese Academy of Sciences, Beijing 100049, China
[4] Key Laboratory of Optical Astronomy, National Astronomical Observatories, Chinese Academy of Sciences, Beijing 100012, China

Received 2015 December 16; accepted 2016 April 14

Abstract In this paper, a cascade acceleration feedback control (AFC) enhanced by a disturbance observation and compensation (DOC) method is proposed to improve the tracking precision of telescope systems. Telescope systems usually suffer some uncertain disturbances, such as wind load, nonlinear friction and other unknown disturbances. To ensure tracking precision, an acceleration feedback loop which can increase the stiffness of such a system is introduced. Moreover, to further improve the tracking precision, we introduce the DOC method which can accurately estimate the disturbance and compensate it. Furthermore, the analysis of tracking accuracy used by this method is proposed. Finally, a few comparative experimental results show that the proposed control method has excellent performance for reducing the tracking error of a telescope system.

Key words: telescopes — instrumentation: control method – instrumentation miscellaneous: high angular resolution – instrumentation: detector — control software

1 INTRODUCTION

Telescopes are playing increasingly important roles in many fields, such as ground-based space observation (Valyavin et al. 2014), optical communication (Sodnik et al. 2010; Khalighi & Uysal 2014) and quantum communication (Gisin & Thew 2010). Tracking precision is a key indicator of telescope systems and determines the performance of a given telescope system. However, it is inevitable that telescope systems will suffer some unknown nonlinear disturbances that will severely reduce tracking precision and pointing precision. Examples include wind load (Qiu et al. 2014), friction (De Wit et al. 1995) and other disturbances (Su et al. 2015). Usually, because the volume taken up by a telescope system is relatively large, wind load is the major external disturbance (Qiu et al. 2014). Especially when there is no dome, or the dome of the telescope is opened, it is important to minimize the influence of wind disturbance. Obviously, the classical control structure (a double loop that controls both position and speed) may not guarantee enough tracking precision. At present, to reduce the influence of external disturbances, there are mainly the following control methods that could be chosen: robust control (Nicol et al. 2008), adaptive control (Yao et al. 2014), active disturbance rejection control (Cai et al. 2015), disturbance observation and compensation (DOC) (He & Ge 2015) and internal model control (Canale et al. 2009).

In recent years, with advancements in electronic devices, an accelerometer has become an important sensor in control systems. The cascade acceleration loop has also been used in some high precision systems, such as telescope systems (Sedghi et al. 2008; Tang et al. 2009; Ge et al. 2015), missile control systems (Chwa 2014), and robots (Koch et al. 2013; Xu et al. 2000). An acceleration loop can enhance the stiffness of a system, while rejecting a disturbance. However, the current ability is still not adequate for high performance in telescopic systems (Sedghi et al. 2008; Tang et al. 2009).

In this paper, a new control method which combines acceleration feedback control (AFC) with the DOC method is proposed. This approach makes use of the acceleration feedback constituting the acceleration loop for increasing the stiffness of telescope systems, and uses the DOC for estimating and compensating an external disturbance. As is well known, the DOC needs an approximate mathematical model for the system. The compensation precision depends on the accuracy of the associated approximate mathemati-

cal model. However, the wind disturbance is a kind of relatively low frequency disturbance (Emde et al. 2003), so it is easy to accurately measure low frequency characteristics of the system. To illustrate the excellent performance of the proposed control method, three comparative experiments will be described in this article. The remainder of this paper is organized as follows: Section 2 highlights the dynamic models. Sections 3 and 4 introduce the controller design and the theory behind the analysis method used, respectively. Experimental results are presented in Section 5. Finally, some conclusions are provided in Section 6.

2 DYNAMIC MODELS

In most telescope systems, the control structure is usually a double loop structure (DLS), which includes the velocity loop and the position loop. The velocity loop is used to increase the ability for inhibiting disturbances and enhance the stiffness of the system. The position loop is used to guarantee tracking accuracy. However, even though the velocity loop can increase the ability for inhibiting disturbances, it can hardly eliminate unknown external disturbances. Therefore, it will be difficult to further enhance the precision of the system.

This section mainly analyses the performance of three control methods: the DLS, the cascade AFC method and the cascade AFC with DOC (AFC-DOC)

A telescope system is usually a two-axis structure, such as an azimuth axis and an elevation axis as shown in Figure 1.

The dynamics of the tracking system are described by Equation (1)

$$\begin{aligned} \frac{d\theta(t)}{dt} &= \omega(t); \frac{\omega(t)}{dt} = a(t); \\ Ja(t) &= u - B\omega(t) - f(t,\omega); \\ u &= k_t i, \quad J = J_m + J_l, \quad T_m = u. \end{aligned} \tag{1}$$

In Equation (1), J_m and J_l are the motor inertia and the load inertia, respectively. θ and ω represent the load angle and angle velocity, respectively. T_m represents the torque applied at the motor. i is the current to the motor. $f(t,\omega)$ represents all the uncertain disturbances, including interior disturbances and external disturbances. B is the viscous coefficient.

According to Equation (1), the transfer function $G(s)$ from the input u to the output acceleration a is described by Equation (2)

$$G(s) = \frac{a(s)}{u(s)} = \frac{s}{Js + B}\,. \tag{2}$$

2.1 DLS

The classical control structure of the telescope is depicted in Figure 2 and the closed-loop velocity is given by Equation (3).

$$\omega = \frac{C_\omega G\frac{1}{s}}{1 + C_\omega G\frac{1}{s}}\omega_{\mathrm{ref}} + \frac{H\frac{1}{s}}{1 + C_\omega G\frac{1}{s}} f. \tag{3}$$

In Equation (3), ω is angular speed. G is the controlled object. C_ω is a term that controls the speed. ω_{ref} is the given speed which is sent to a speed loop. $H(S)$ is the transfer function that defines a relation from a disturbance torque to gimbal acceleration. In the low frequency domain, $H(S)$ is just a gain.

Similarly, according to the control scheme, the encoder reading θ will be given by Equation (4).

$$\theta = \frac{C_\omega G\frac{1}{s^2}}{1 + C_\omega G\frac{1}{s}} C_p(\theta_{\mathrm{ref}} - \theta) + \frac{H\frac{1}{s^2}}{1 + C_\omega G\frac{1}{s}} f. \tag{4}$$

So,

$$\theta = \frac{C_p C_\omega G\frac{1}{s^2}}{1 + C_\omega G\frac{1}{s} + C_p C_\omega G\frac{1}{s^2}}\theta_{\mathrm{ref}} + \frac{H\frac{1}{s^2}}{1 + C_\omega G\frac{1}{s} + C_p C_\omega G\frac{1}{s^2}} f. \tag{5}$$

Let F_{PSD} be the power spectral density (PSD) of the disturbance. From the above equations, we can find that the PSD of the angular position θ is

$$\theta_{\mathrm{PSD}} = \left| \frac{H \cdot \frac{1}{s^2}}{1 + C_\omega G \cdot \frac{1}{s} + C_p C_\omega G \cdot \frac{1}{s^2}} \right|^2 F_{\mathrm{PSD}}. \tag{6}$$

From this equation, we can conclude that the performance of the control system depends on the velocity loop controller and the position loop controller, but especially on the velocity loop controller. When designing an appropriate controller, there will be a minimum θ_{PSD}, which minimizes the effect caused by the disturbance f.

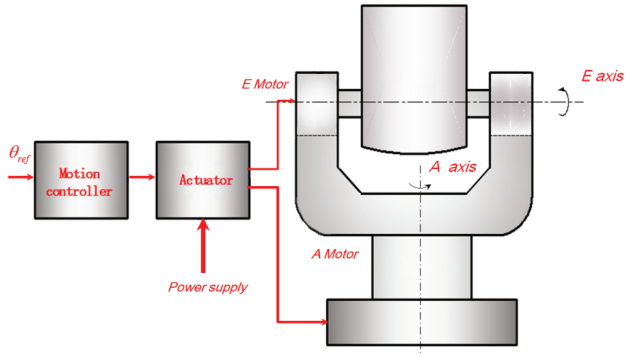

Fig. 1 The gimbal structure and servo system of a telescope.

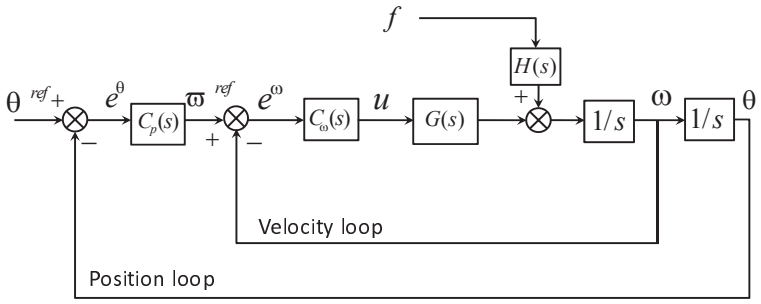

Fig. 2 The classical DLS scheme.

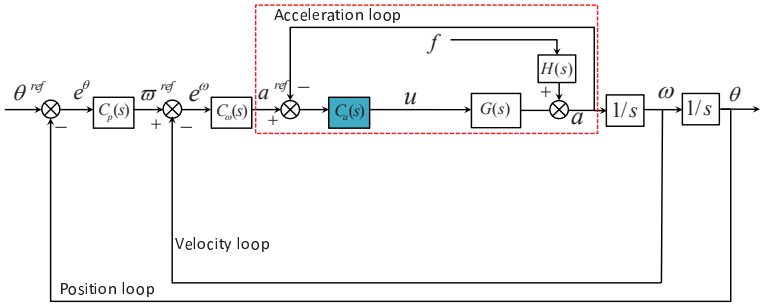

Fig. 3 The AFC scheme.

2.2 AFC

The AFC scheme is depicted in Figure 3.

The closed loop angular position θ is given by

$$\theta = \frac{C_p C_\omega C_a G \cdot \frac{1}{s^2}}{1 + C_a G + C_\omega C_a G \cdot \frac{1}{s} + C_p C_\omega C_a G \cdot \frac{1}{s^2}} \theta_{\text{ref}} + \frac{H \cdot \frac{1}{s^2}}{1 + C_a G + C_\omega C_a G \cdot \frac{1}{s} + C_p C_\omega C_a G \cdot \frac{1}{s^2}} f \,. \tag{7}$$

Then

$$\theta_{\text{PSD}} = \left| \frac{H \cdot \frac{1}{s^2}}{1 + C_a G + C_\omega C_a G \cdot \frac{1}{s} + C_p C_\omega C_a G \cdot \frac{1}{s^2}} \right|^2 F_{\text{PSD}}. \tag{8}$$

As Equation (8) shows, the performance of AFC depends on the acceleration loop controller, the velocity loop controller and the position loop controller, but especially on the acceleration loop controller. The disturbance rejection ability of AFC is stronger than that of DLS.

2.3 AFC-DOC

From Figure 4, it is easy to get

$$\begin{aligned} a &= \Big[(a_{\rm ref}-a)C_a - C_{fd}(a-u\tilde{G})\Big]G + fH, \\ a &= uG + fH. \end{aligned} \tag{9}$$

It can be shown that $u = (a - fH)G^{-1}$, then substitution yields

$$a = \Big[(a_{\rm ref}-a)C_a - C_{fd}(a - aG^{-1}\tilde{G} + fHG^{-1}\tilde{G})\Big]G + fH. \tag{10}$$

For $G^{-1} = 1/G$, this can be easily implemented in low frequency, so

$$a = C_aGa_{\rm ref} - C_aGa - C_{fd}Ga + C_{fd}\tilde{G}a - C_{fd}\tilde{G}fH + fH, \tag{11}$$

$$a = \frac{C_aG}{1 + C_aG + C_{fd}(G-\tilde{G})}a_{\rm ref} + \frac{(1-C_{fd}\tilde{G})H}{1 + C_aG + C_{fd}(G-\tilde{G})}f. \tag{12}$$

For $a_{\rm ref} = (\omega_{\rm ref} - \omega)C_\omega$, the closed velocity ω will be

$$\omega = \frac{C_aG}{1 + C_aG + C_{fd}(G-\tilde{G})}(\omega_{\rm ref}-\omega)C_\omega \cdot \frac{1}{s} + \frac{(1-C_{fd}\tilde{G})H}{1 + C_aG + C_{fd}(G-\tilde{G})}f \cdot \frac{1}{s}, \tag{13}$$

$$\omega = \frac{C_\omega C_aG}{1 + C_aG + C_{fd}(G-\tilde{G}) + C_\omega C_aG \cdot \frac{1}{s}}\omega_{\rm ref} \cdot \frac{1}{s} + \frac{(1-C_{fd}\tilde{G})H}{1 + C_aG + C_{fd}(G-\tilde{G}) + C_\omega C_aG \cdot \frac{1}{s}}f \cdot \frac{1}{s}. \tag{14}$$

Simultaneously, for $\omega_{\rm ref} = (\theta_{\rm ref} - \theta)C_p$, the closed angular position θ will be

$$\theta = \frac{C_pC_\omega C_aG}{1 + C_aG + C_{fd}(G-\tilde{G}) + C_\omega C_aG \cdot \frac{1}{s}}(\theta_{\rm ref}-\theta) \cdot \frac{1}{s^2} + \frac{(1-C_{fd}\tilde{G})H}{1 + C_aG + C_{fd}(G-\tilde{G}) + C_\omega C_aG \cdot \frac{1}{s}}f \cdot \frac{1}{s^2}, \tag{15}$$

$$\begin{aligned} \theta \;=\; & \frac{C_pC_\omega C_aG}{1 + C_aG + C_{fd}(G-\tilde{G}) + C_\omega C_aG \cdot \frac{1}{s} + C_pC_\omega C_aG \cdot \frac{1}{s^2}} \cdot \frac{1}{s^2}\theta_{\rm ref}, \\ & + \frac{(1-C_{fd}\tilde{G})H}{1 + C_aG + C_{fd}(G-\tilde{G}) + C_\omega C_aG \cdot \frac{1}{s} + C_pC_\omega C_aG \cdot \frac{1}{s^2}} \cdot \frac{1}{s^2}f. \end{aligned} \tag{16}$$

From Equation (16), the PSD of the angular position θ is

$$\theta_{\rm PSD} = \left|\frac{(1-C_{fd}\tilde{G})H \cdot \frac{1}{s^2}}{1 + C_aG + C_{fd}(G-\tilde{G}) + C_\omega C_aG \cdot \frac{1}{s} + C_pC_\omega C_aG \cdot \frac{1}{s^2}}\right|^2 F_{\rm PSD}. \tag{17}$$

3 DESIGN CONTROLLER

Our telescope system is a 1.2 m telescope which is shown in Figure 5. This telescope is used for quantum laser communication between ground and a satellite, but it is also used for astronomical observation. The sensors for gimbal control include grating ruler, velocity measuring gyroscope and accelerometer.

The goal of the controller is to eliminate external disturbances as much as possible. Since measurement of the disturbance and the compensation controller need an approximate mathematical model of the system, the dynamic characteristic of the object which is between the input current and output acceleration should be obtained. This can be performed by a spectral analyzer. The open loop response to the input current and the output acceleration are shown in Figure 6.

As Figure 6 shows, by the method of curve fitting, we can derive a mathematical model that approximates the behavior of the system. Because the telescope system mainly suffers some low frequency disturbances (Emde et al. 2003), the high frequency part of the mathematical model of the system can be neglected. Therefore, the model that describes the behavior of the system can be approximated by the curve fit method as

$$\tilde{G} \approx \frac{2.25}{0.011s + 1}. \tag{18}$$

So, we can derive

$$\tilde{G}^{-1} \approx \frac{0.011s + 1}{2.25}. \tag{19}$$

Combining the control scheme block and the above analysis, it can be found that a low pass filter and a gain should be designed in the controller, so

$$C_{fd} = \frac{k_a s + a}{s + a}. \tag{20}$$

A classical PI controller can be chosen in the acceleration loop.

$$C_a = k_p^a \Big[a_{\rm ref}(t) - a(t)\Big] + k_i^a \int\limits_0^t \Big[a_{\rm ref}(\tau) - a(\tau)\Big] d\tau\,. \tag{21}$$

The k_p^a and k_i^a are the proportional gain and the integral gain of the acceleration loop controller, respectively.

When the compensation controller and the acceleration loop controller are completed, observations that test disturbance rejection ability can be performed.

Figure 7 shows the measured response from the current disturbance to the tracking error (by imposing a disturbance on the internal current loop of the drive power amplifier). As shown, when the DLS method is adopted, the disturbance rejection ratio is about -5dB at 0.6 Hz. When the AFC method is adopted, the disturbance rejection ratio is -35 dB at 0.6 Hz. When the AFC-DOC method is adopted, the disturbance rejection ratio is about -55 dB at 0.6 Hz. This indicates that the proposed AFC-DOC method will have the best disturbance rejection ability.

The disturbance rejection ratio is a relative value which depends on the feedback gain to the dynamic signal analyzer. In this experiment, the closed-loop bandwidth of speed loops of three control methods is almost the same, about 12 Hz.

According to the above control scheme, in the velocity loop and the position loop, the classical PI controller will be chosen.

$$\begin{aligned} a_{\rm ref} &= k_p^{\omega}\big[\omega_{\rm ref}(t) - \omega(t)\big] + k_i^{\omega} \int\limits_0^t \big[\omega_{\rm ref}(\tau) - \omega(\tau)\big] d\tau, \\ \omega_{\rm ref} &= k_p^{\theta}\big[\theta_{\rm ref}(t) - \theta(t)\big] + k_i^{\theta} \int\limits_0^t \big[\theta_{\rm ref}(\tau) - \theta(\tau)\big] d\tau. \end{aligned} \tag{22}$$

4 PERFORMANCE ANALYSIS

From the above equations, we can conclude the following:

(1) When the DLS is applied, the PSD of position will be

$$\theta^1_{\rm PSD} = \left| \frac{H \cdot \frac{1}{s^2}}{1 + C_\omega G \cdot \frac{1}{s} + C_p C_\omega G \cdot \frac{1}{s^2}} \right|^2 F_{\rm PSD}. \tag{23}$$

(2) When the control structure is the AFC, the PSD of position will be

$$\theta^2_{\rm PSD} = \left| \frac{H \cdot \frac{1}{s^2}}{1 + C_a G + C_\omega C_a G \cdot \frac{1}{s} + C_p C_\omega C_a G \cdot \frac{1}{s^2}} \right|^2 f_{\rm PSD}. \tag{24}$$

(3) When the control structure is the AFC-DOC, the PSD of position will be

$$\theta^3_{\rm PSD} = \left| \frac{(1 - C_{fd}\tilde{G}) H \cdot \frac{1}{s^2}}{1 + C_a G + C_{fd}(G - \tilde{G}) + C_\omega C_a G \cdot \frac{1}{s} + C_p C_\omega C_a G \cdot \frac{1}{s^2}} \right|^2 f_{\rm PSD}. \tag{25}$$

If the design DOC controller obeys the relation

$$C_{fd} \cong 1/\tilde{G}, \tag{26}$$

then

$$\theta^3_{\rm PSD} \to 0. \tag{27}$$

This will lead to the condition

$$\theta^3_{\rm PSD} = \min\Big\{\theta^1_{\rm PSD}, \theta^2_{\rm PSD}, \theta^3_{\rm PSD}\Big\}. \tag{28}$$

In Equation (28), it can be seen that the PSD of the position is the least when the AFC-DOC method is applied, which means that the system will suffer the least influence from external disturbances.

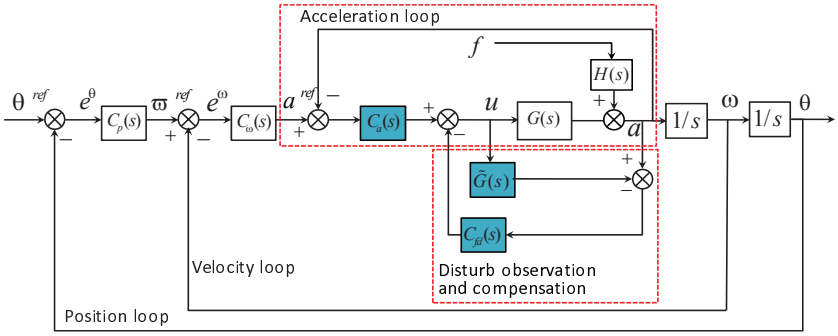

Fig. 4 The AFC-DOC scheme.

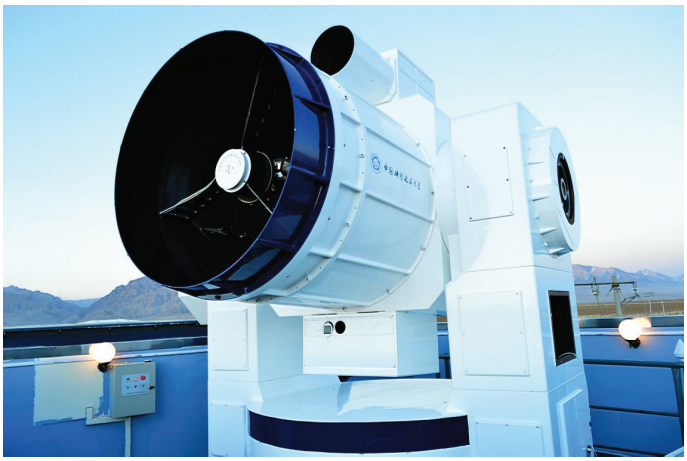

Fig. 5 The 1.2 m telescope system used for quantum communication and astronomical observation.

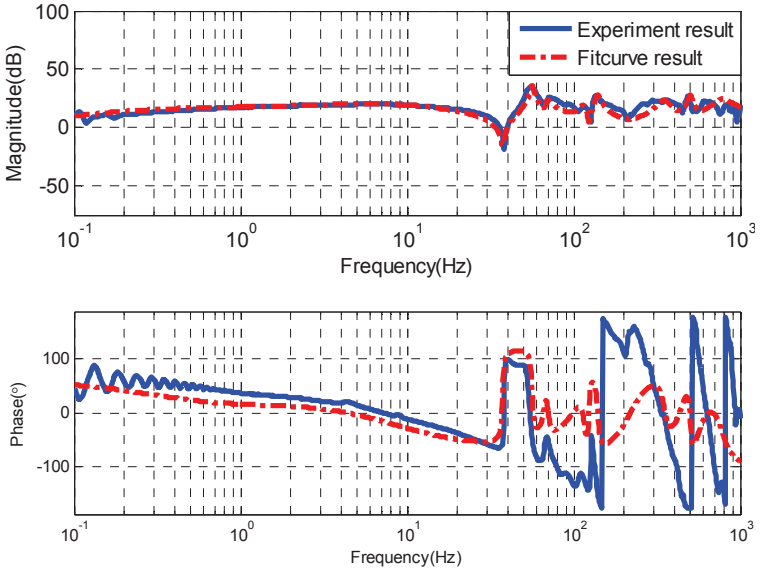

Fig. 6 The open loop response from the input current to the output acceleration.

5 EXPERIMENTAL SETUP AND RESULTS

Verification experiments are applied to the azimuth axis of the 1.2 m telescope system. The main hardware consists of a direct drive torque motor, an angular encoder with an accuracy of about 0.53 arcsecond in terms of root mean square (RMS), and a pair of linear accelerometers with a resolution of about 0.00005 g. The speed information was taken from the difference shown by the encoder rather than a tachometer.

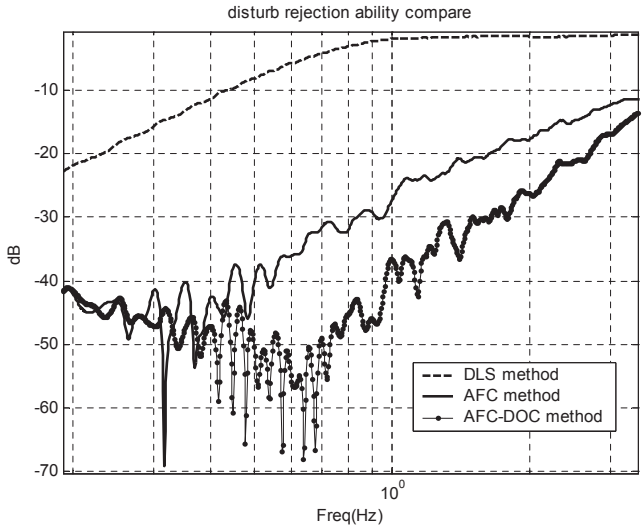

Fig. 7 A comparison of the results of disturbance rejection ability.

Fig. 8 The pull and push dynamometer.

Fig. 9 Imposing some periodic disturbance torques via a dynamometer.

To verify the disturbance rejection ability, a pull and push dynamometer is chosen to introduce some disturbances. Meanwhile, the disturbance torque is measured by a dynamometer by which we impose the torque on the gimbal. The disturbance torque is transferred to a recording computer via a USB cable. In Figure 4, the input of $C_{fd}(s)$ is the observed acceleration disturbance which is proportional to torque disturbance at low frequency.

Figure 8 shows the pull and push dynamometer which is chosen. In Figure 9, some periodic pull and push disturbances are imposed on the azimuth axis of the telescope system via the dynamometer. The following three experiments are compared:

(1) The DLS: without the acceleration loop, it only needs to include the velocity loop controller and the position loop controller.
(2) The AFC: an acceleration loop controller is added in the system. The acceleration signal can be measured by the accelerometer.
(3) The AFC-DOC: as Figure 4 shows, the DOC controller is in the inner part of the acceleration loop.

The three control methods are tested at a fixed azimuth position. Then a periodic pull and push torque disturbance is imposed on the azimuth axis; the magnitudes are about $\pm 300\,\mathrm{N\,m}$. Simultaneously, the data of periodic disturbances are recorded by a computer. From Figures 10, 12 and 14, the periods and magnitudes of disturbances which are applied in the system can be seen. The result is calibrated according to the torque imposed on the gimbal in the DLS method experiment.

In Figure 11, it can be seen that the system will have a larger tracking error, when the DLS method is used. The RMS of tracking error is $2.89''$ while the RMS of the disturbance is $131.8\,\mathrm{N\,m}$, which indicates that the DLS method has the lowest inhibiting ability for an external disturbance.

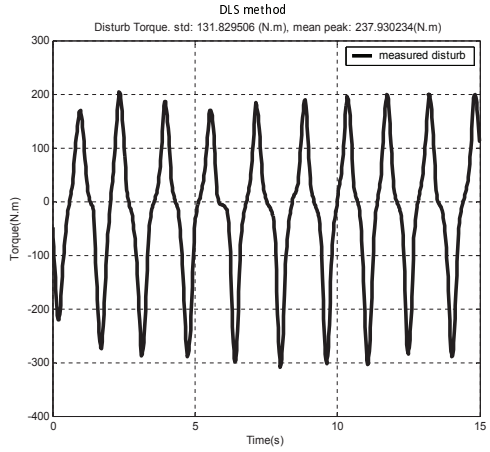

Fig. 10 The measured disturbance torque in the experiment that implements the DLS method.

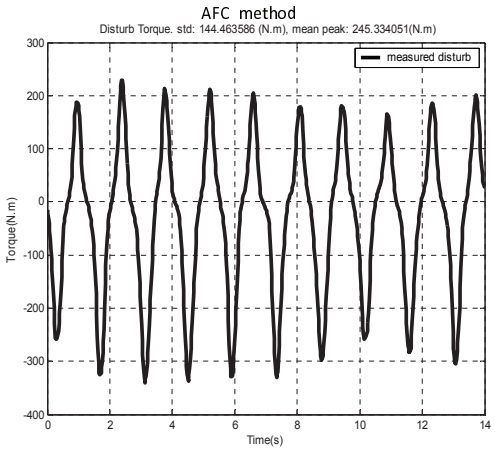

Fig. 12 The measured disturbance torque in the experiment with the AFC method.

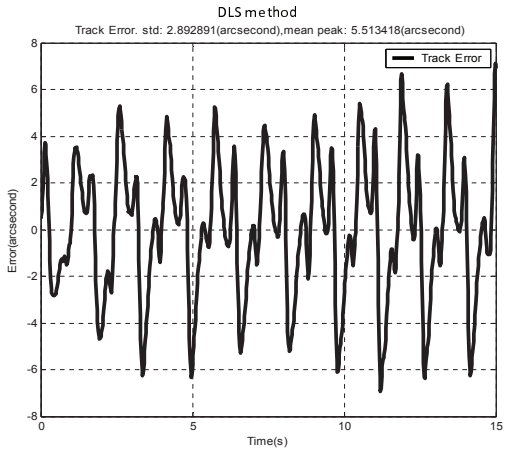

Fig. 11 The tracking error with the DLS method.

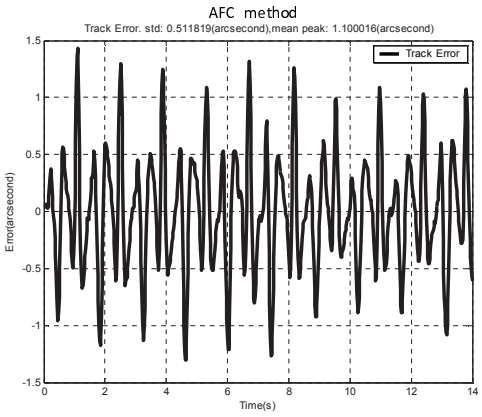

Fig. 13 The tracking error with the AFC method.

In Figure 12, the RMS of tracking error is about $0.51''$ while the RMS of disturbance is 144.5 N m, when the AFC method is applied in the system. Comparatively speaking, the AFC-DOC has the least disturbance error. In Figure 15, the RMS of tracking error is only $0.23''$ but the RMS of the disturbance is 140.9 N m.

Simultaneously, in Figure 14, it can be seen that the applied disturbance torque can be estimated by the DOC method. The dashed line is the torque disturbance which is estimated by the DOC method. The solid line is the disturbance torque applied to the system which is measured by the dynamometer. This shows that the cascade AFC-DOC method can accurately estimate the disturbance and compensate for it, leading to minimized tracking error. In Equation (28), it also shows that the PSD of the tracking error is the least. In Figure 16, the tracking error of three control methods is compared.

In Table 1, the statistical data of tracking error and disturbance torque from three experiments are listed. The tracking error is calibrated to apply disturbance torque to the experiment with the DLS method.

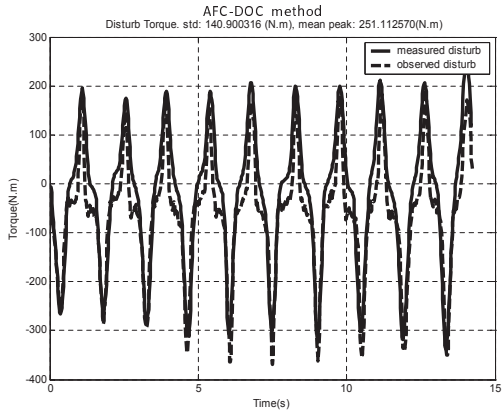

Fig. 14 The measured and estimated disturbance torque in the experiment with the AFC-DOC method.

6 DISCUSSION

Uncertainties in the external disturbances have been the major factor which restricts the performance of a telescope's tracking control systems. This is because the sys-

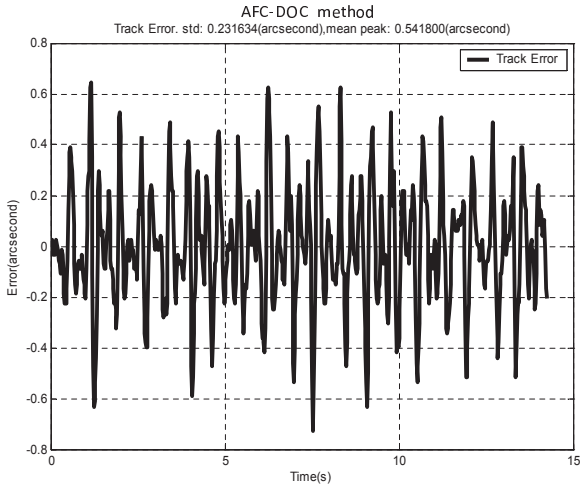

Fig. 15 The tracking error with the AFC-DOC method.

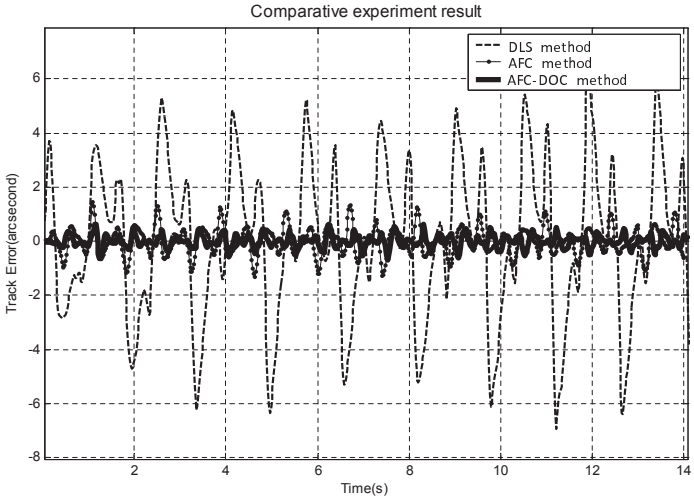

Fig. 16 Comparison of the experimental results for tracking errors.

Table 1 The Experimental Result of Three Controllers

	DLS	AFC	AFC-DOC
RMS of disturbance	131.8 N m	144.5 N m	140.9 N m
mean $\|peak\|$ of disturbance	237.9 N m	245.3 N m	251.1N m
RMS of tracking error	$2.89''$	$0.51''$	$0.23''$
mean $\|peak\|$ of tracking error	$5.51''$	$1.1''$	$0.54''$
RMS of tracking error calibrated to disturbance	$2.89''$	$0.47''$	$0.22''$
mean $\|peak\|$ of tracking error calibrated to disturbance	$5.51''$	$1.07''$	$0.51''$

Notes: The "mean $|peak|$" is the mean absolute value of the peaks; Calibration is applied to the value of the "DLS"method.

tem's tracking precision decreases when it suffers some uncertain nonlinear disturbances. Therefore, to reduce the influence from the disturbances, an AFC-DOC method is proposed in this paper. The acceleration loop can increase the stiffness of a system. The DOC method can accurately estimate disturbance and compensate it. The combination of the two control methods increases the ability of the system to inhibit external disturbances. Finally, the experimental results show that the proposed control method has excellent performance for improving the tracking precision of the telescope system.

The DOC method is restricted by the precision of the mathematical model describing the gimbal and the noise of the accelerometer. From Figure 14, when the external torque changes direction, the error between the real torque and the estimated torque is obvious. This is mainly because of the hysteresis lag between the pull and push of the dynamometer, especially when static friction takes effect.

Acknowledgements This work was supported by the Quantum Communication Project, one of the Strategic Pilot Projects, Chinese Academy of Sciences. We acknowledge the use of the newly constructed Delingha (Qinghai province) 1.2 m telescope, Nanshan (Xinjiang province) 1.2 m telescope and Xinglong (Hebei province) 1.0 m telescope. The control method is applied to those telescopes, especially the two newly constructed telescopes. Special thanks go to Zuo-Wei Lv (as shown in Fig.9), Xiao-Ming Huang and Zhi-Qiang Wang.

References

Cai, H.-X., Huang, Y.-M., Du, J.-F., et al. 2015, Mathematical Problems in Engineering, 501, 701510

Canale, M., Fagiano, L., & Vecchio, C. 2009, 47th IEEE Transactions on Intelligent Transportation Systems, 10, 31

Chwa, D. 2014, IEEE Transactions on Aerospace Electronic Systems, 50, 2369

De Wit, C. C., Olsson, H., Astrom, K. J., & Lischinsky, P. 1995, Automatic Control, IEEE Transactions on, 40, 419

Emde, P., Suss, M., Eisenträger, P., Moik, R., & Karcher, H. 2003, in Proc. SPIE, 5179, Optical Materials and Structures Technologies, ed. W. A. Goodman, 282

Ge, L., Lu, X.-M., & Jiang, X.-J. 2015, RAA (Research in Astronomy and Astrophysics), 15, 1077

Gisin, N., & Thew, R. T. 2010, Electronics letters, 46, 965

He, W., & Ge, S. S. 2015, Mechatronics, IEEE/ASME Transactions on, 20, 237

Khalighi, M. A., & Uysal, M. 2014, Communications Surveys & Tutorials, IEEE, 16, 2231

Koch, H., Konig, A., Weigl-Seitz, A., Kleinmann, K., & Suchy, J. 2013, Instrumentation and Measurement, IEEE Transactions on, 62, 268

Nicol, C., Macnab, C., & Ramirez-Serrano, A. 2008, in Proceedings of the Canadian Conference on Electrical and Computer Engineering, 1233

Qiu, D., Sun, M., Wang, Z., Wang, Y., & Chen, Z. 2014, Control Systems Technology, IEEE Transactions on, 22, 1983

Sedghi, B., Bauvir, B., & Dimmler, M. 2008, in Proc. SPIE, 7012, Ground-based and Airborne Telescopes II, 70121Q

Sodnik, Z., Furch, B., & Lutz, H. 2010, Selected Topics in Quantum Electronics, IEEE Journal of, 16, 1051

Su, Y., Wang, Q., Yan, F., Liu, X., & Huang, Y. 2015, Mathematical Problems in Engineering, 2015

Tang, T., Huang, Y., Fu, C., & Ma, J. 2009, in 4th International Symposium on Advanced Optical Manufacturing and testing Technologies: Large Mirrors and Telescopes, International Society for Optics and Photonics, 72810F

Valyavin, G., Bychkov, V., Yushkin, M., et al. 2014, Astrophysical Bulletin, 69, 224

Xu, W., Han, J., & Tso, S. 2000, Mechatronics, IEEE/ASME Transactions on, 5, 292

Yao, J., Jiao, Z., & Ma, D. 2014, Industrial Electronics, IEEE Transactions on, 61, 3630